Quantifying the Hurricane Catastrophe Risk to Offshore Wind Power

Stephen Rose[a], Paulina Jaramillo[a], Mitchell J. Small[a,b], Jay Apt[a,c]

[a] Department of Engineering & Public Policy, Carnegie Mellon University, Pittsburgh PA 15213, USA

[b] Department of Civil & Environmental Engineering, Carnegie Mellon University, Pittsburgh PA 15213, USA

[c] Tepper School of Business, Carnegie Mellon University, Pittsburgh PA 15213, USA

E-mail addresses: srose@cmu.edu (S. Rose), pjaramil@andrew.cmu.edu (P. Jaramillo) , ms35@andrew.cmu.edu (M. Small), apt@cmu.edu (J. Apt)

Abstract

The U.S. Department of Energy has estimated that over 50 GW of offshore wind power will be required for the United States to generate 20% of its electricity from wind. Developers are actively planning offshore wind farms along the U.S. Atlantic and Gulf coasts and several developers have signed leases for offshore sites. These planned projects will be located in areas that are sometimes struck by hurricanes. We present a method to estimate the catastrophe risk to offshore wind power using simulated hurricanes. Using this method, we estimate the fraction of offshore wind power offline simultaneously and the cumulative damage in a region. In Texas, the most vulnerable region we studied, 11% of offshore wind power could be offline simultaneously due to hurricane damage with a 100-year return period and 5% could be destroyed in any 10-year period. We also estimate the risks to single wind farms in four representative locations; we find the risks are significant but lower than those estimated in previously published results. Much of the hurricane risk to offshore wind turbines can be mitigated by designing turbines for higher maximum wind speeds, ensuring that turbine nacelles can turn quickly to track the wind direction even when grid power is lost, and building in areas with lower risk.

1. BACKGROUND

As a result of state renewable portfolio standards and federal tax incentives, there is growing interest and investment in renewable sources of electricity in the United States. Wind is the renewable resource with the largest installed-capacity growth in the last 5 years, with U.S. wind power capacity increasing from 8.7 GW in 2005 to 47 GW in 2011.[1] All of this development has occurred onshore. U.S. offshore wind resources may also prove to be a significant contribution to increasing the supply of renewable, low-carbon electricity. The National Renewable Energy Laboratory (NREL) estimates that offshore wind resources can be as high as four times the 2010 U.S. electricity generating capacity.[2] Although this estimate does not take into account siting, stakeholder, and regulatory constraints, it indicates that U.S. offshore wind resources are significant. No offshore wind projects have been developed in the United States, but there are 10 offshore wind projects in the planning process (with an estimated capacity of 3.8 GW)[1] and more proposed[3]. The U.S. Department of Energy's 2008 report, *20% Wind by 2030* envisions 54 GW of shallow offshore wind capacity to optimize delivered generation and transmission costs.[4]

The U.S. has good wind resources along the Atlantic, Pacific, and Great Lake coasts. Many areas along the Atlantic Coast and Gulf Coast are particularly attractive because they have high average wind speeds, are in relatively shallow water, and are close to major population centers. Unconstrained resources at depths shallower than 30 m in the Atlantic coast, from Georgia to Maine, are estimated to be 345 GW; the estimate for these resources in the Gulf of Mexico (Texas and Louisiana) is 198 GW.[2] For comparison, the 2010 net summer generation capacity for the entire U.S. was 1,039 GW.[5]

Offshore wind turbines in these areas will be at risk from Atlantic hurricanes. Between 1949 and 2006, 93 hurricanes struck the U.S. mainland according to the HURDAT (Hurricane Database) database of the National Hurricane Center.[6] Only 15 years in this 58-year period did not incur insured hurricane-related losses.[7] Wind turbines are vulnerable to hurricanes because the maximum wind speeds in those storms can exceed the design limits of wind turbines. In 2003, a wind farm of seven utility-scale turbines in Okinawa, Japan, was destroyed by typhoon Maemi, which had an estimated maximum sustained wind speed of 60 m/s[8] (equivalent to a Category 4 hurricane), and several turbines in China were damaged by typhoon Dujuan.[9]

It is rare but not unprecedented for a single natural disaster to damage multiple conventional power plants. Hurricane Katrina flooded critical pumps and controllers at one power plant, and damaged cooling tower shrouds and fans at several others.[10] Hurricane Sandy in 2012 may have damaged several gas turbine power plants in New Jersey[11]. The Tohoku earthquake and tsunami in March 2011 caused significant damage to the Fukushima Daiichi and Daini power stations; four reactors at Fukushima Daiichi, totaling 2,719 MW of capacity, were permanently shut down.[12] The earthquake and tsunami also damaged several large coal power plants: 6,050 MW of capacity were offline after the earthquake, 4,250 MW were still offline in July 2011, and 2,000 MW (the Haramachi Power Station) were expected to be offline until the summer of 2013.[13,14] Interestingly, the Kamisu semi-offshore wind farm was struck by a 5-meter tsunami during the Tohoku earthquake but resumed operation three days later when the local electrical grid was re-established.[15]

Hurricane effects on offshore wind power may be more similar to damage to the electrical transmission system than damage to conventional power plants. Like the components of the transmission system, offshore wind turbines are geographically dispersed and operate independently.

Severe weather events, such as hurricanes[10] and ice storms[16], sometimes damage individual transmission components, which in turn can cause blackouts. However, repairing damage to offshore wind turbines will likely take much longer and require more specialized equipment than repairing damages to the transmission system. Many transmission system components are commodities and are often stockpiled before hurricane seasons, but most wind turbine components are built-to-order and offshore wind turbine repairs require specialized ships and cranes.

Previous work by Rose, *et al*, estimated the hurricane risk to a single wind farm over its lifetime using compound probability distributions fitted to one hundred years of historical hurricane records.[17] That study likely over-estimates the risk to a wind farm because it assumes that any hurricane making landfall in a county affects the entire coastline of that county with its maximum winds, but the area of maximum winds is typically smaller than a coastal county in the U.S.[18] Furthermore, that method did not consider hurricane tracks, so it could not assess the correlated risk to nearby wind farms. The new work we present here calculates the correlated risk to all wind farms in a region by analyzing thousands of simulated hurricanes and accounting for the wind field of each hurricane.

The research presented in this paper follows a catastrophe modeling approach.[19] We construct a hazard model that describes the frequency of occurrence, intensity, and location of hurricanes that make landfall in the continental U.S. We also create an inventory of wind turbines at risk by placing simulated turbines in offshore locations likely to be developed. Finally, we model the vulnerability of the wind turbines to hurricane winds.

2. METHOD

We calculate the distribution of wind power offline due to hurricane damage by simulating fifty 5,000-year periods of hurricane activity along the U.S. coast (a total of 2.5×10^5 years). Each hurricane is generated by a statistical-deterministic model developed by Emanuel, *et al*.[20] We calculate the wind field of each hurricane to determine the wind speed at each turbine location, and use a probabilistic damage function to determine whether each turbine buckles. This method differs from the one developed by Rose, *et al*[17], because that previous method calculated hurricane rates of occurrence and intensities by fitting probability distributions to historical hurricanes and did not model the wind field. After towers buckle, we assume it takes several years to rebuild them in case several hurricanes strike the same area in a short period (for example, seven hurricanes made landfall in Florida in 2004-5, with two each year striking the same area). Using simulated hurricanes allows us to base our risk calculations on much longer periods of hurricane activity than are available in historical records, which reduces the uncertainty of our estimates. However, we explicitly model uncertainties in hurricane size and rate of occurrence, and the turbine damage function.

2.1 Simulated Hurricanes

The historical record of hurricanes in the U.S. is insufficient to confidently estimate the risk of intense hurricanes. For this reason, we estimate the risk using hurricanes simulated with the method of Emanuel, *et al*, that generates hurricanes with statistical properties that agree with the historical record.[20] Emanuel's method simulates hurricanes by first randomly seeding weak vortices randomly in space and time.[21] Those vortices follow a track stochastically determined by ambient winds, and their intensity evolves along that track as a deterministic function of wind and ocean conditions known as the Coupled Hurricane Intensity Prediction System (CHIPS); some vortices grow into hurricanes but most dissipate.[22]

We generate 300 tropical cyclones that make landfall in the continental U.S. based on climatological conditions for each year from 1979-2011, for a total of 9,900 storms. This range of years covers periods of low hurricane activity in the continental U.S. (e.g. 1981-2, 2000-1) and periods of high activity (e.g. 1985, 2004-2005)[6] as well as several El Niño/La Niña cycles. The 3,285 storms that reach hurricane intensity within 200 km of the continental U.S. are the pool of hurricanes we draw randomly from when we create long time series of hurricane activity. For each hurricane, we calculate the maximum 1-minute sustained wind speed at each offshore wind turbine location using the wind profile proposed by Holland, *et al.*[23] The wind profile depends on the radius of maximum wind r_{max}. We scale the CHIPS-calculated r_{max} value for each hurricane by a lognormal-distributed random variable (described in *Hurricane Size* below) to make the distribution of radii similar to the distribution of radii of historical hurricanes. The maximum sustained wind speed we calculate for each hurricane is the sum of the circular wind speed, a fraction of the of the wind speed at 850 hPa height, and a latitude-dependent fraction of the hurricane's translation speed.[24]

2.2 Historical Hurricanes

We use the historical data for north Atlantic hurricanes to check the results calculated with the simulated hurricanes above. The historical record we use consists of the Extended Best Track data set for 1988-2011[25] combined with the HURDAT data set for 1900-1987[6]. The Extended Best Track data includes estimates of the radius of maximum wind r_{max} for each hurricane but HURDAT does not, so we estimate missing r_{max} values from minimum central pressure, if available, using the following formula given by Powell, *et al*,[26] in (1):

$$r_{max} = \frac{1}{1.852}\exp(2.0633 + 0.0182\Delta_p - 0.00019008\Delta_p^2 + 0.0007336\phi^2 + \epsilon) \quad (1)$$

where the factor of 1/1.852 converts from nautical miles to km, Δ_p is the difference between ambient pressure (1,013 hPa) and minimum central pressure, ϕ is latitude, and ε is a normally-distributed error term with mean of 0 and standard deviation of 0.3. When pressure is not available, we assume a radius of maximum wind of 33 km, the historical median for landfalling hurricanes in the continental US given by Ho, *et al.*(27)

2.3 Wind Farm Placement

We place offshore wind turbines in all feasible locations along the U.S. East Coast and Gulf Coast (Figure 1). We define "feasible locations" as locations with suitable wind resource between 8 and 93 km (5 – 50 nautical miles) from shore with water shallower than 30 m, similar to the definition used in the Eastern Wind Integration and Transmission Study (EWITS).[28] We follow the definition of "suitable wind resource" used in EWITS: average annual wind speed at 80 m sufficient for a typical IEC Class II turbine to have a capacity factor of at least 32% (approximately 7.4 m/s at 90-m height). The wind resource data are taken from maps created by the National Renewable Energy Laboratory (NREL), scaled from 90 m to 80 m height with a power law exponent of 1/7. We exclude marine sanctuaries, military practice areas, Navy aviation warning areas, shipping lanes, active oil and gas leases, and bays and inland waterways. References for the wind resource and exclusion area databases are given in the online Supporting Information. The turbines are placed with a density of 5 MW/km^2, equivalent to a spacing of approximately 8 rotor diameters between turbines for the NREL 5MW reference turbine; for comparison, turbines at the Horns Rev I wind farm west of Denmark are spaced 7 rotor diameters apart.[29]

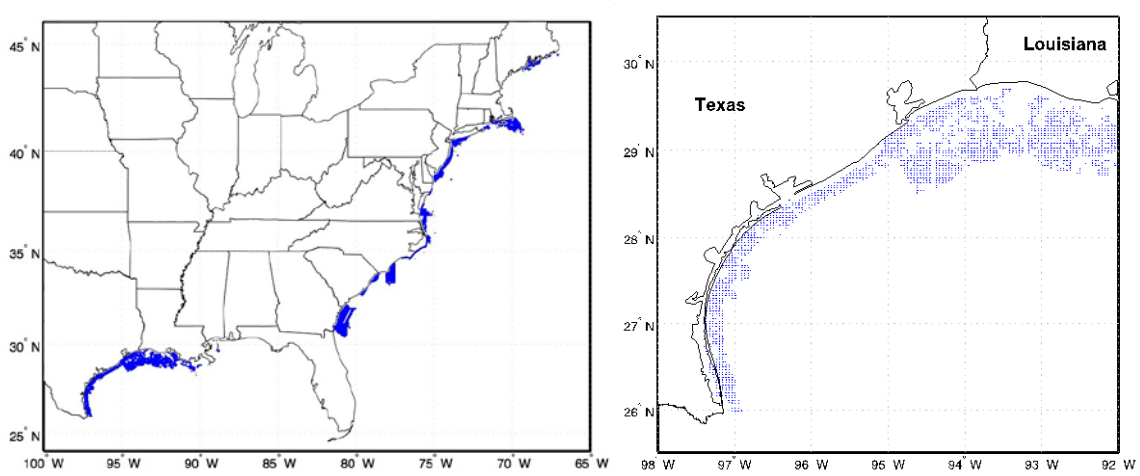

Figure 1: Wind turbine locations for the "Full Development" scenario. Mississippi, Alabama, and Florida are excluded because wind resource estimates are not available for those states. Detail of the wind turbine location map for Texas and western Louisiana, showing excluded areas such as shipping lanes and oil and gas leases.

The turbines are grouped into four regions in order to aggregate damages from individual hurricanes: Texas, the Southeast (Georgia, South Carolina, and North Carolina), the Mid-Atlantic (Virginia, Maryland, Delaware, New Jersey, and New York), and New England (Rhode Island, Massachusetts, New Hampshire, and Maine).

2.4 Rate of Hurricane Occurrence

The number of U.S.-landfalling hurricanes in our 5000-year simulations is drawn from a cyclic nonhomogeneous Poisson process. Emanuel's method[20], which generates the pool of simulated hurricanes (described above) also generates a Poisson rate parameter Λ_m for each of the 33 years of climatological conditions: m = [1979, 1980, … , 2011]. We cyclically repeat those 33 rate parameters so that there is a rate parameter corresponding to each of the 5000 years in the periods of hurricane activity we simulate: [Λ_{1979}, Λ_{1980}, … , Λ_{2011}, Λ_{1979}, Λ_{1980}, …]. To determine the number of hurricanes that make landfall in each year of the simulation, we draw from a Poisson distribution with the corresponding rate parameter.

The value of the rate parameter Λ_m is uncertain because it is calculated from a finite number of storms. We model this uncertainty as a Bayesian posterior distribution with an informationless prior. The posterior for the Poisson distribution is a gamma distribution with shape hyperparameter t_m and rate hyperparameter k_m: $\Lambda_m \sim \text{Gamma}(t_m, k_m)$. The hyperparameter k_m is the number of U.S.-landfalling hurricanes in the climatological conditions of year m. The hyperparameter t_m is number of years for k_m lanfalling hurricanes to occur; we calculate this as the number of storms seeded in the climatological conditions of year m divided by a universal constant that relates the storm seeding rates with global historical genesis rates.[21] To simulate the number of hurricanes in a year of a 5000-year simulation, we first draw a realization λ from the corresponding gamma-distributed random variable Λ_m, and then we draw the number of hurricanes from a Poisson distribution with the rate parameter λ.

2.5 Hurricane Size

The radius of maximum wind r_{max} of each simulated hurricane is calculated deterministically by the CHIPS model[30] from climatological conditions . However, we find those r_{max} values tend to be smaller and more narrowly distributed (Figure 2B) than the r_{max} values of comparable hurricanes in

the historical record (Figure 2A). Therefore we scale the r_{max} values of the simulated hurricanes by a lognormal-distributed random variable S so that the distribution of their scaled r_{max} values (Figure 2C) better matches the distribution for historical hurricanes.

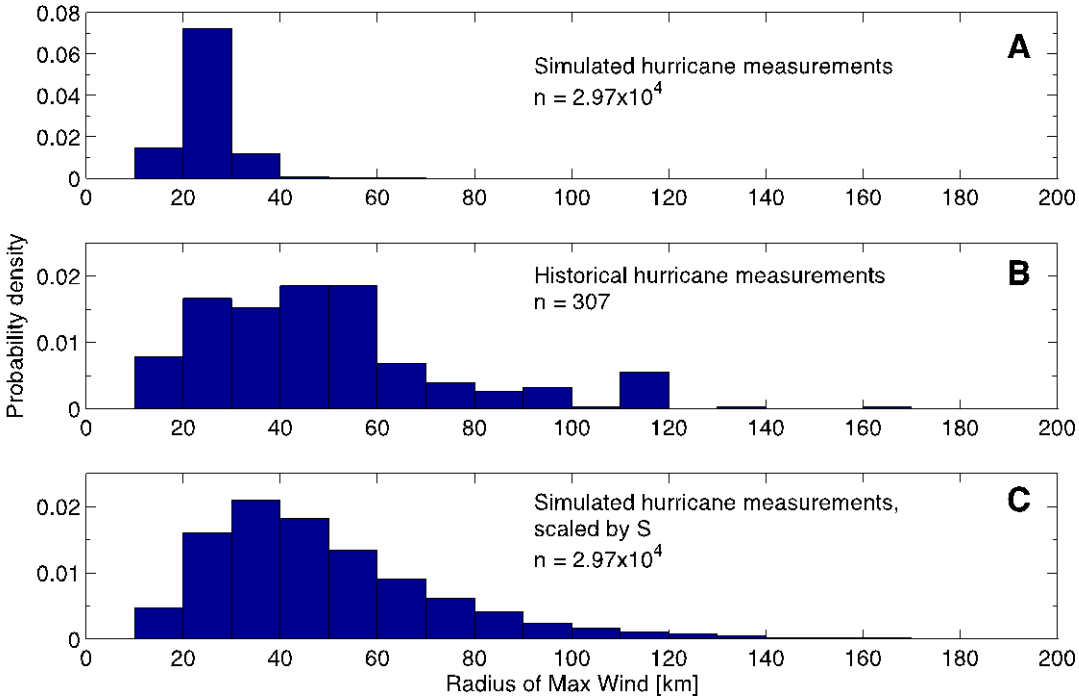

Figure 2: Histogram of radius of maximum winds for hurricanes within 200 km of the continental U.S. coast. The distribution of r_{max} in (C), has been scaled by a lognormal distribution described in "Hurricane Size" to match the distribution of r_{max} for historical hurricanes in (B) better than the r_{max} calculated by Emanuel's CHIPS model shown in (A).

We calculate the lognormally-distributed scaling factor $S = H/M$, where H is a lognormal distribution fit to r_{max} of historical hurricanes from the Extended Best Track data set for 1988-2010[25] and M is a lognormal distribution fit to r_{max} of the simulated hurricanes described above. The distributions for both H and M are fitted to only hurricanes within 200 km of the continental U.S. coast.

The distributions H and M are uncertain because they are fitted to a finite number of hurricane size measurements. We model these uncertainties as Bayesian posterior distributions with informationless priors[31]. The posterior for the joint distribution of normal distribution parameters μ and θ (where the precision $\theta = 1/\sigma^2$) is a normal-gamma distribution with three hyperparameters calculated from sufficient statistics: α is the number of observations of r_{max}, β is the sum of the observed r_{max} values, and γ is the sum of the square of the observed r_{max} values. The marginal distribution for θ is shown in (2) and conditional distribution for μ given θ is shown in (3).

$$\theta \sim \text{Gamma}\left(\frac{\alpha\gamma - \beta^2}{2\alpha}, \frac{\alpha+1}{2}\right) \quad (2)$$

$$\mu|\theta \sim \text{Normal}\left(\frac{\beta}{\alpha}, \frac{1}{\alpha\theta}\right) \quad (3)$$

We use the posterior for a normal distribution because lognormal distributions use the same parameters as the corresponding normal distribution. The hyperparameter values for r_{max} measurements 2 hours apart for historical hurricanes within 200 km of the continental U.S. coast are: $\alpha_H = 479$, $\beta_H = 1.83\text{x}10^3$, $\gamma_H = 7.17\text{x}10^3$ and the hyperparameters for r_{max} measurements 2 hours apart for simulated hurricanes within 200 km of the continental U.S. coast are: $\alpha_M = 40337$, $\beta_M = 1.30\text{x}10^5$, $\gamma_M = 4.19\text{x}10^5$.

We limit the scaled radius of maximum winds to the range 18.5 - 98.9 km based on the observed 5th and 95th percentile values in the Extended Best Track data set for 1988-2010 within 200 km of the U.S. coast (409 observations for 41 hurricanes).[25] These limits are comparable to the r_{max} values that meet quality control standards in the analysis by Willoughby, *et al*[32], and the limits on Powell's expression for r_{max} as a function of central pressure and latitude[26].

2.6 Model Validation for Hurricane Occurrence and Wind Speeds

In order to validate the simulated hurricane activity we use in this paper, we calculate the return period of tropical storms, hurricanes, and intense hurricanes at 45 locations along the Gulf and Atlantic coasts to compare to return periods calculated from historical hurricanes for the same locations by Keim, *et al*[33], and we calculate return periods for a range of wind speeds for New Orleans and Miami to compare to results presented by Emanuel and Jagger.[34] The results, which are presented in the online Supporting Information, show that the model we develop here predicts return periods for intense hurricanes (≥ Category 3) similar to return periods calculated from the historical record.

2.7 Wind Turbine Damage Function

We calculate the probability of a single turbine tower buckling as a function of the maximum 10-minute sustained wind speed it experiences at hub height. This damage function is similar to that used by Rose, *et al*[17], but we modify it here by adding normally-distributed scatter around the log-logistic function to better represent the uncertainty in fitting the function to simulated turbine buckling data (Figure 3). The parameters of the damage function used here (given in Table I) are calculated from simulations of the NREL 5-MW offshore reference turbine design[35]; we expect other turbine designs will have damage functions with similar forms but different parameters. This damage function does not account for wave loads or damage mechanisms other than tower buckling.

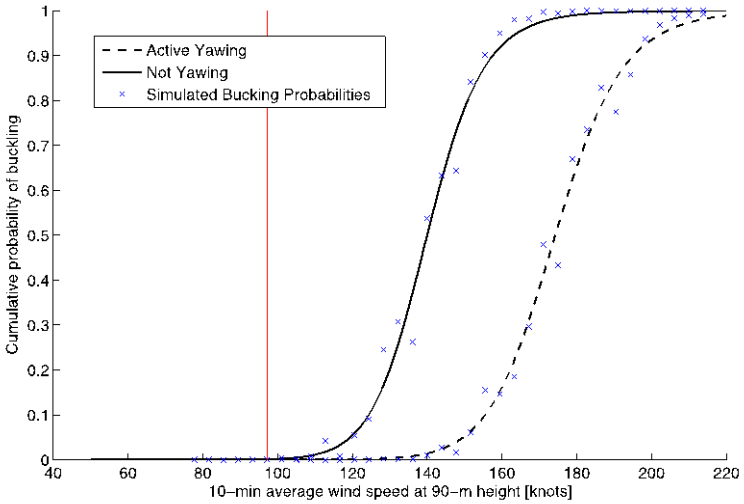

Figure 3: Log-logistic functions fitted to probability of tower buckling as a function of wind speed. The vertical red line at 95 knots is the 10-minute sustained wind speed with a 50-year return period used to design Class I wind turbines in the IEC 61400-3 standard.

The hurricane wind field model calculates 1-minute sustained wind speed but our damage function is based on 10-minute sustained wind speed; we divide the 1-minute speed by a factor of 1.11 to get 10-minute sustained speed, as suggested by Harper, *et al*[36].

The probability of a wind turbine tower buckling $D(u)$ as a function of 10-minute average hub-height wind speed u is calculated as a log-logistic function with normally-distributed scatter, described by equation (4) and equation (5) and the parameters in Table I.

$$D(u) \sim \text{Normal}\left(\text{loglogistic}(u;\ \alpha, \beta), \sigma_D\right) \quad (4)$$

$$\text{loglogistic}(u;\ \alpha, \beta) = \frac{(u/\alpha)^{\beta}}{1 + (u/\alpha)^{\beta}} \quad (5)$$

The parameters α, β, σ_D are fit to probabilities of turbine tower buckling calculated by comparing simulated stresses on a 5-MW offshore wind turbine designed by the U.S. National Renewable Energy Laboratory[35] to the stochastic resistance to buckling proposed by Sørensen, *et al.*[37] The simulations are described in more detail by Rose, *et al.*[17] The predictive distribution given in (4) is fitted to simulations of wind turbine buckling at 36 10-min average wind speeds from 77.8 – 213.8 knots (40 – 110 m/s, in 2 m/s steps) using Metropolis-Hastings (MH) sampling, a special case of Markov Chain Monte Carlo (MCMC) methods[38]; additional detail is given in the online Supporting Information. We give summary statistics for the empirical distribution of each parameter from MH sampling in Table I considering two load cases: a non-yawing turbine hit broadside by the wind and a yawing turbine hit head-on by the wind.

Table I: Descriptive statistics for the parameters of the predictive distribution for the wind turbine damage function, which models the probability that a turbine will buckle at a given 10-min average wind speed *u*. These parameters are fit to simulations of wind turbine shut down with blades feathered. **(p < 0.05), *(p < 0.01)**

		Mean	Median	Std. Dev.	Correlation coefficients for α, β, σ_D
Non-yawing turbine (broadside to wind)	α (scale)	139.6	139.6	0.455	$\begin{bmatrix} 1 & & \\ -0.072^{**} & 1 & \\ 0.000 & 0.070^{**} & 1 \end{bmatrix}$
	β (shape)	18.6	18.5	0.998	
	σ_D (std. dev.)	0.0356	0.0352	0.0044	
Yawing turbine (head-on to wind)	α (scale)	174.0	174.0	0.842	$\begin{bmatrix} 1 & & \\ 0.086^{***} & 1 & \\ 0.113 & 0.119^{***} & 1 \end{bmatrix}$
	β (shape)	19.6	19.6	0.411	
	σ_D (std. dev.)	0.0295	0.0292	0.0038	

3. RESULTS

3.1 Wind Power Simultaneously Offline

We estimate the return periods for fractions of the wind power in a region simultaneously offline due to hurricane damage for fifty 5,000-year periods. The return period is the inverse of the annual probability of a given fraction of wind power being offline. We assume it takes 2 years to rebuild turbines buckled by hurricanes, so the damage from multiple hurricanes within 2 years is cumulative; we plot the sensitivity of the results to rebuilding time in Figure 6. In Texas (Figure 4) the median amount of wind power offline with a 100-year return period is 11% with a range of 8.3– 16% for non-yawing turbines. For a 50-year return period, the median fraction offline is 6.3% with a range of 4.7 – 8.1%. If the turbines were able to yaw to track the wind direction, the median amount of wind power offline in Texas is 0.37% with a 100-year return period and 0.10% with a 50-year return period. In the Southeast (GA, SC, and NC), shown in Figure 5, the median amount of wind power offline with a 100-year return period is 1.9%, with a range of 1.2% – 3.0% for non-yawing turbines. For a 50-year return period in the Southeast, the median fraction offline is 0.65% with a range of 0.38 – 0.98%. We do not show results for the Southeast if turbines were able to yaw; the median wind power offline is 0.01% with a 100-year return period and 0% with a 50-year return period. We also do not show results for the Mid-Atlantic and New England because the risks are too small to estimate with the 3,285 simulated landfalling hurricanes we used in our simulations.

Our damage model predicts that historical hurricanes would have been similarly destructive if offshore wind turbines had existed in the locations we describe above. The most destructive would have been Hurricane Carla, which struck Texas in 1961. It would have buckled 7.9% of the turbines

(6.8 GW) in Texas if they were unable to yaw and 0.4% (0.38 GW) if they could yaw fast enough to always point into the wind. Similarly, Hurricane Helene in 1958 would have destroyed 1.8% of the non-yawing turbines (1.8 GW) in the Southeast and Hurricane Gloria in 1985 would have destroyed 0.2% of the non-yawing turbines (0.1 GW) in the Mid-Atlantic. The one exception is Hurricane Gerda in 1969, which would have destroyed 8.8% of the non-yawing turbines (3.4 GW) in New England, significantly more than our simulations predict for even a 1,000-year return period (we predict a median of 1.5% and maximum of 4.2%). For comparison, the only other historical hurricane that would have caused measureable simulated damage in New England was Hurricane Esther in 1961, which would have destroyed 0.2% (0.08 GW) of the non-yawing turbines.

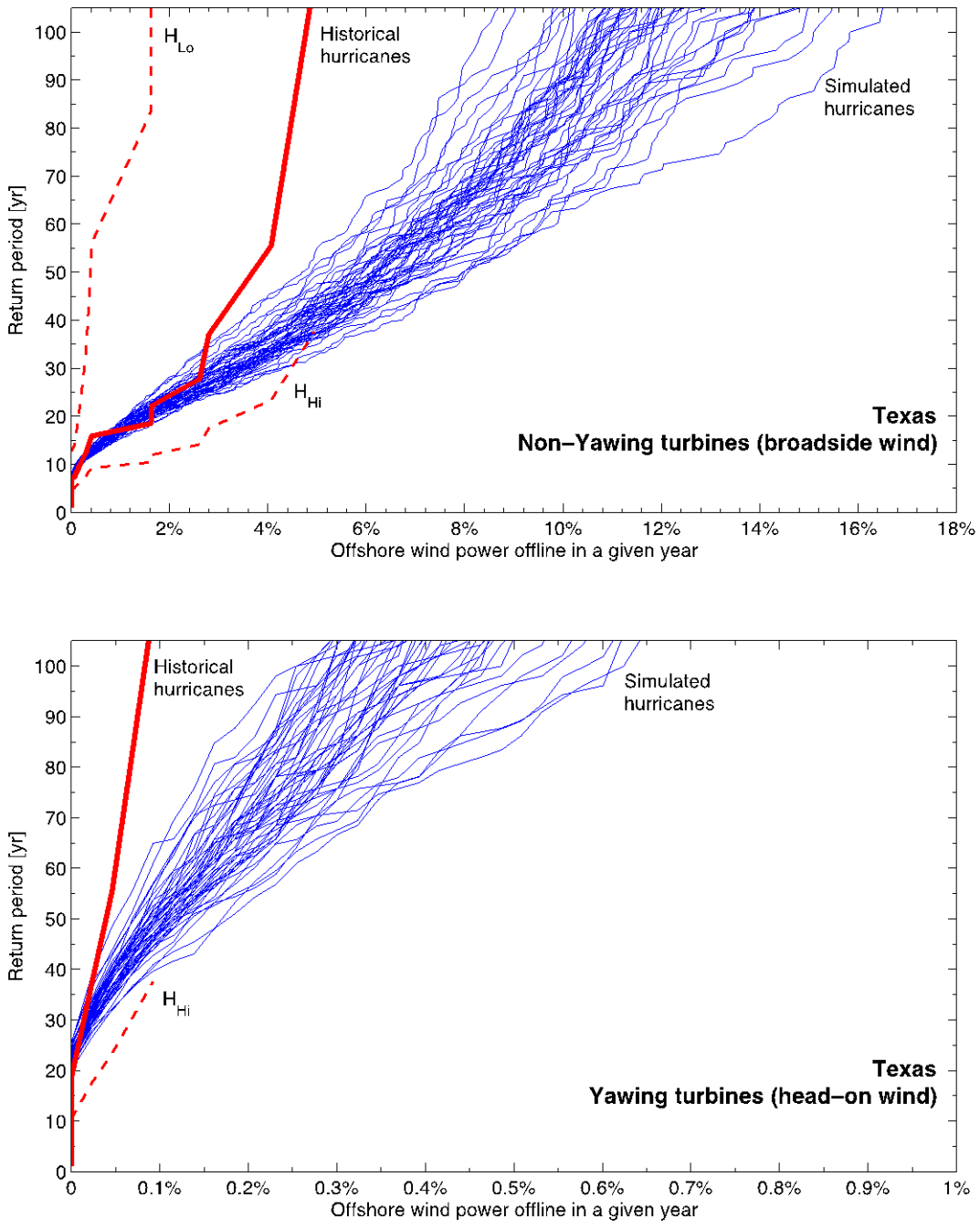

Figure 4: Return period for fraction of wind power offline due to hurricane damage in the Texas, assuming turbines are placed in all locations described above (total capacity of 87 GW). The top plot gives risks for non-yawing turbines; the bottom gives risks for yawing turbines. Each of the "Simulated hurricanes" lines represents one of the fifty 5,000-year periods of simulated hurricanes. The "Historical hurricane" line represents risk calculated from the historical hurricane record (1900 - 2011) and "H_{Lo}" and "H_{Hi}" represent the lower and upper confidence bounds for the historically-based estimates.

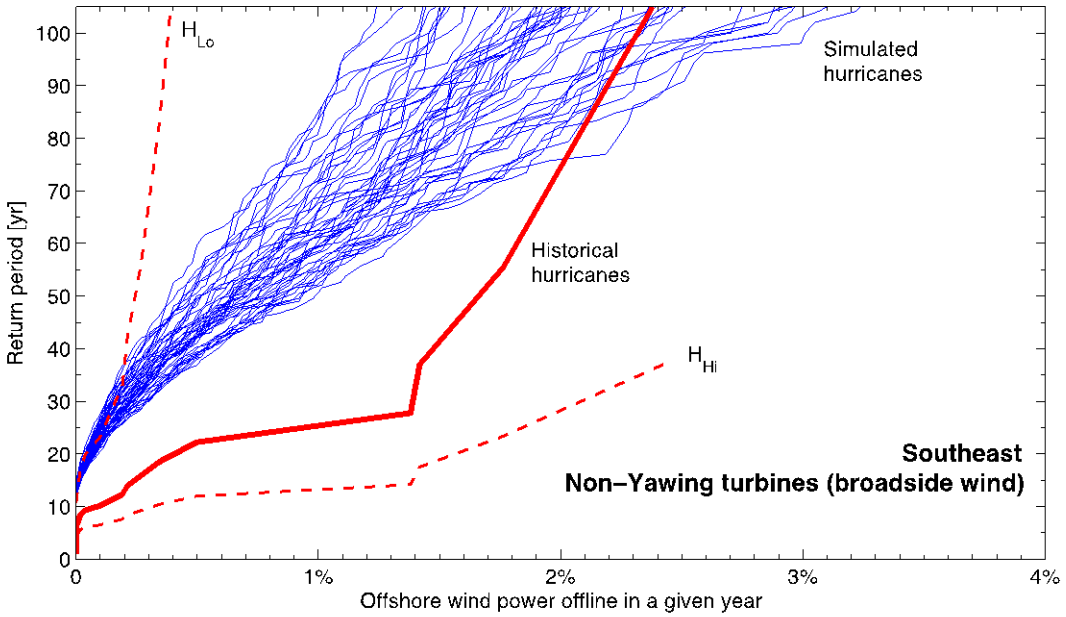

Figure 5: Return period for fraction of wind power offline due to hurricane damage in the Southeast (GA, SC, NC), assuming turbines are placed in all locations described above (total capacity of 104 GW) and the turbines cannot yaw. We do not show the results for yawing turbines because the risks are negligible. Each of the "Simulated hurricanes" lines represents one of the fifty 5,000-year periods of simulated hurricanes. The "Historical hurricane" line represents risk calculated from the historical hurricane record (1900 - 2011) and "H_{Lo}" and "H_{Hi}" represent the lower and upper confidence bounds for the historically-based estimates.

The lines labeled "Historical hurricanes" in Figure 4 and Figure 5 show damage that would have been caused by historical hurricanes if offshore turbines had existed in the locations we describe above. The lines labeled H_{Lo} and H_{Hi} represent the lower and upper confidence bounds for the empirical CDF of historically-based risks, calculated using Greenwood's formula[39].

These results are most sensitive to the uncertainty in the size of hurricanes and the turbine rebuilding time. Sensitivity of wind power simultaneously offline to rebuilding time is shown in Figure 6 for the 100-year return period in Texas.

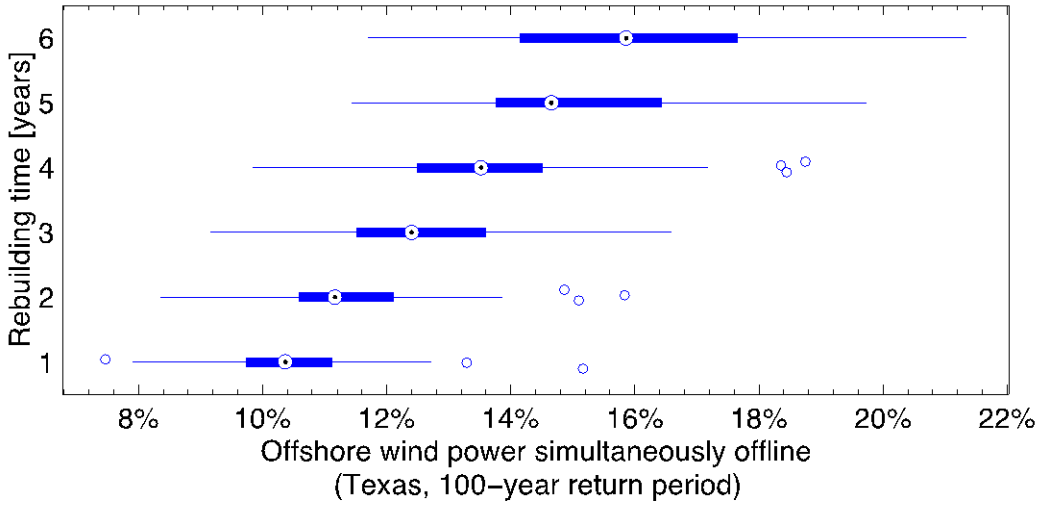

Figure 6: Sensitivity of results to rebuilding time. These results are the percentage of Texas offshore wind power simultaneously offline with a 100-year return period. The boxes represent the 25th and 75th percentiles of the simulation results, the whiskers represent the maximum extent of the simulated predictions not classed as outliers, and circles are the outliers.

3.2 Cumulative damage

In the previous section, we showed that only a small fraction of offshore wind power in a region would be offline simultaneously due to buckling by hurricanes. However, the cumulative damage over several years can be significantly larger. We estimate the cumulative damage to offshore wind power in each region and in the entire eastern U.S. for periods of 2, 5, and 10 years, assuming turbines designed to existing standards. The results, plotted in Figure 7, show that the cumulative damage increases with the length of the period and that Texas is likely to see the most cumulative damage.

For Texas and the entire Atlantic coast except Florida ("All U.S."), we predict a 10% probability that more than 0.7% of offshore wind power will be destroyed in any 2-year period, more than 2.9% in any 5-year period, and more than 5.7% in any 10-year period if the turbines cannot yaw. For Texas alone, there is a 10% probability that more than 0.9% of offshore wind power will be destroyed in any 2-year period, more than 4.8% in any 5-year period, and more than 10% in any 10-year period if the turbines cannot yaw. For the Southeast (GA, SC, NC), there is a 90% probability that more than 0.04% of offshore wind power will be destroyed in any 2-year period, more than 0.5% in any 5-year period, and more than 1.6% in any 10-year period if the turbines cannot yaw. If the turbines can yaw to point directly into the wind, the cumulative damages are lower by at least a factor of 10. We do not show results for the Mid-Atlantic and New England because the simulated cumulative damages are too small to estimate with the 3,285 simulated landfalling hurricanes we used in our simulations.

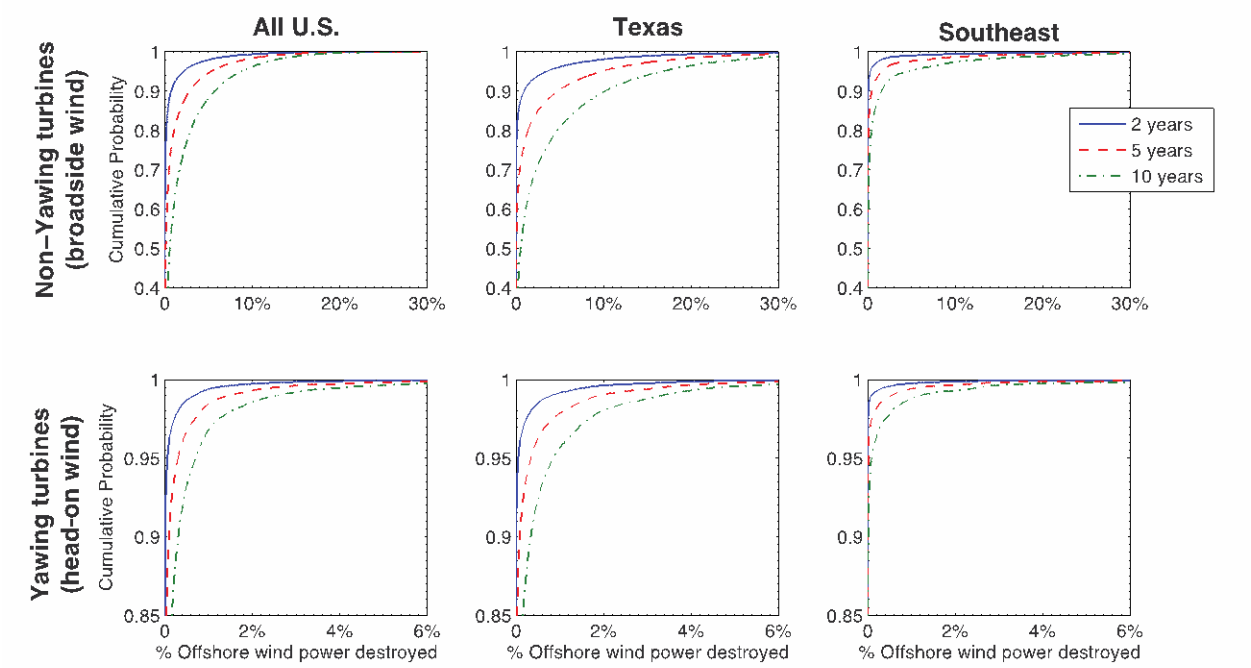

Figure 7: Predicted cumulative fraction of offshore wind turbines destroyed in periods of 2, 5, and 10 years. The top row shows cumulative damage for non-yawing turbines and the bottom row for yawing turbines. The left-most column shows cumulative damage for the entire eastern U.S. coast, the center column for Texas, and the right-most column for the Southeast region (GA, SC, NC).

3.3 Lifetime Risk to a Single Wind Farm

We estimate the lifetime hurricane risk to a single wind farm in four locations: Galveston County, TX; Dare County, NC; Atlantic County, NJ; Dukes County, MA. For each location, we calculate the lifetime risk as the distribution of the simulated number of turbine towers buckled by hurricanes in 20 years, the typical design life of wind turbines, if buckled turbines are not replaced. For each county, we simulate 5×10^4 years of hurricane activity at several possible offshore wind farm locations using hurricanes simulated with a method proposed by Emanuel, *et al*[20]; the exact wind farm locations are given in the online Supporting Information. The results for Galveston and Dare counties are shown in Figure 8 and Figure 9, where the lines plot the median risk for all periods and all wind farm sites near a particular county; the error bars represent the 5th and 95th percentile risks. Solid lines plot the risk to non-yawing turbines and dashed lines plot the risk to yawing turbines. Results for Atlantic and Dukes counties are given in the online Supporting Information.

We present these results (labeled "New results (this paper)") for comparison with results for the same four locations presented in Rose, *et al*,[17] (labeled "Rose, *et al*") and a correction of those earlier results that converts 1-min average wind speeds to 10-min average wind speeds, described in Rose, et al[40] (labeled "Rose, *et al*, corrected"). There are several important differences between the methods used in the current paper and the methods for previous results. First, the new results are based on the simulated hurricanes described above; previous results are based on probability distributions fitted to historical hurricanes. Second, the new results model the wind field of a hurricane near shore, whereas the previous did not. Third, the new results correct an error in the previous results described by Powell and Cocke[18] that confused 1-min and 10-min average wind speeds; the results labeled "Rose, *et al*, corrected" correct that error but use probability distributions fitted to historical hurricanes. Table II compares selected results for Galveston, TX calculated with three methods described above; Table III compares selected results for Dare County, NC calculated

with the same three methods. The comparisons in Table II and Table III show that the hurricane risks to offshore wind turbines we predict with the more sophisticated method in this paper are slightly lower than risks predicted by the simplified method developed by Rose, *et al*[17], if the corrections for wind speed averaging period described by Rose, *et al*[40], are applied.

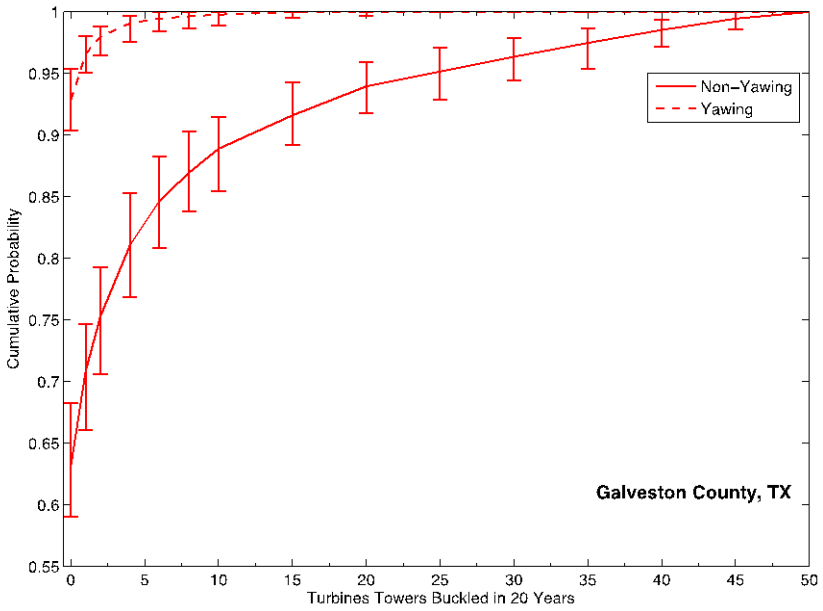

Figure 8: Cumulative distribution of number of turbine towers buckled in Galveston County, TX by hurricanes in 20 years if buckled towers are not replaced. Dashed lines plot the distribution for the case that the turbines can yaw to track the wind direction, and solid lines plot the distribution for the cast that turbines cannot yaw.

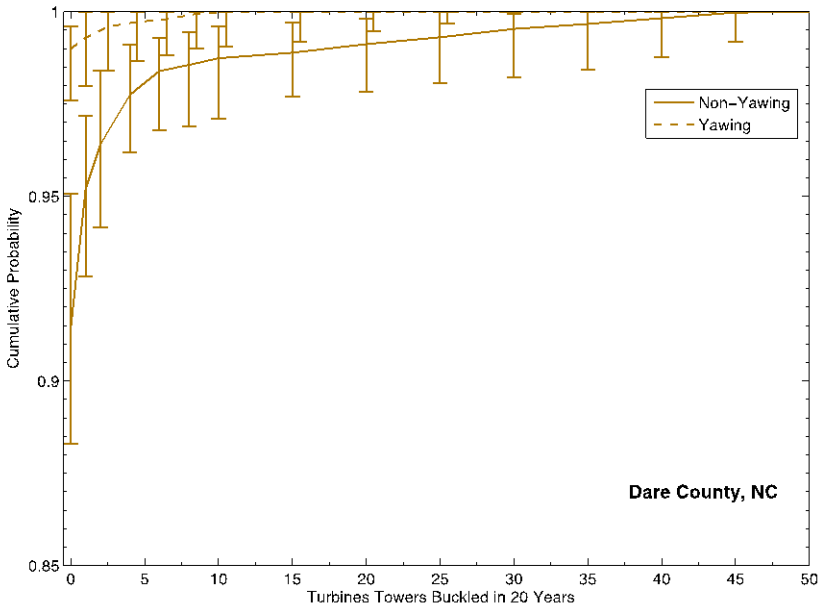

Figure 9: Cumulative distribution of number of turbine towers buckled in Dare County, NC by hurricanes in 20 years if buckled towers are not replaced. Dashed lines plot the distribution for the case that the turbines can yaw to track the wind direction, and solid lines plot the distribution for the cast that turbines cannot yaw.

In Atlantic County, NJ, there is a 0.4 - 3% probability and in Dukes County, MA, a 0.2 – 2% probability that at least one tower will buckle in 20 years if the turbines cannot yaw. The probability of more than half the turbines buckling in the non-yawing case or any turbines buckling in the yawing case in Atlantic County and Dukes County are too small to estimate with the 3,285 simulated landfalling hurricanes we used in our simulations.

Table II: Comparison of results for Galveston County with no rebuilding of buckled turbines.

Galveston County, TX			
		≥ 1 turbine buckled in 20 years	**> 25 turbines buckled in 20 years**
Non-yawing turbine (broadside to wind)	New results (this paper)	32 - 41%	3 – 7%
	Rose, *et al*, corrected[40]	45%	5%
	Rose, *et al*[17]	60%	30%
Yawing turbine (head-on to wind)	New results (this paper)	5 – 10%	0%
	Rose, *et al*, corrected[40]	9%	< 0.1%
	Rose, *et al*[17]	25%	10%

Table III: Comparison of results for Dare County, NC if buckled turbines are not rebuilt.

Dare County, NC			
		≥ 1 turbine buckled in 20 years	**> 25 turbines buckled in 20 years**
Non-yawing turbine (broadside to wind)	New results (this paper)	5 - 12%	0.01 - 2%
	Rose, *et al*, corrected[40]	36%	1%
	Rose, *et al*[17]	60%	9%
Yawing turbine (head-on to wind)	New results (this paper)	0.4 - 2%	< 0.3%
	Rose, *et al*, corrected[40]	5%	< 0.1%
	Rose, *et al*[17]	15%	< 0.1%

4. DISCUSSION

Our results suggest that hurricanes will pose a non-negligible, but likely manageable risk to grid operators in coastal regions should they become dependent on offshore wind power, though hurricanes in the Gulf of Mexico may pose a significant risk to insurers. Grid operators in areas prone to intense hurricanes should account for the hurricane risk when calculating capacity value for offshore wind power if they use existing wind turbine designs. Insurers should carefully assess the spatial and temporal correlation of hurricane risk to offshore wind power in areas prone to intense hurricanes. Hurricane risk can be mitigated by strengthening turbine designs or ensuring that turbines can yaw to track the wind direction even if grid power is lost. These risks may change as the climate changes, but it is unclear whether the risks will increase or decrease.

From the perspective of an electrical grid operator, the hurricane risk to offshore wind power may affect two aspects of electrical grid reliability: system security and system adequacy. Security is a measure of the ability of the power grid to continue operating normally in case of the loss of a major component, such as a power plant or transmission line. The U.S. grid has experience in dealing with temporary losses of major components as a result of hurricanes, and there are established communication protocols that require generators to inform the power grid operators of any generation assets loses.[41] Furthermore, the scale of expected offshore wind power losses, even in extreme events, is similar to the reserve margin used to maintain system security. For example, ERCOT, the Texas grid operator, has a minimum reserve margin target of 13.75% of system load[42], but a 100-year hurricane event would take 9 – 14% of the offshore wind power offline simultaneously.

Adequacy is a measure of the generation and transmission capacity to meet future load. Wind power can contribute only a fraction of its rated power output, known as "capacity value", to system adequacy because wind is a variable resource. There has been significant work on estimating the capacity value of wind power[43-45], but none has considered the risk of losses in wind farm installations resulting from natural hazards. Unlike conventional generators, which can see short-term outages as a result of hurricanes[46], long term loses of offshore wind resources could result from hurricanes. These long-term losses can affect the adequacy of the grid, which in turn would affect security. The results we present in this paper suggests that there is a risk associated with installing significant amounts of offshore wind power in the Gulf of Mexico if the turbines are designed to current standards. Figure 4 shows, for example, that there is a 2% probability of having 4.7 – 8.1% of installed wind capacity offline simultaneously in any given year and a 1% probability of 9 – 14% offline. We thus suggest that methods for calculating the capacity value of offshore wind resources in the Gulf Cost should incorporate the risk of losses due to hurricanes. This will ensure that appropriate long-term reserve margins are maintained and available to maintain security of the grid.

From the perspective of insurers, the hurricane risk to offshore wind power may be significant because offshore turbines are expensive and current turbine designs are vulnerable. For example, a 100-year event (hurricane or series of hurricanes) could cause $31 – 49 billion in damages to offshore wind turbines and a 50-year event could cause $17 – 27 billion if turbines are installed in all feasible locations along the Texas coast (87 GW and assuming an overnight capital cost for offshore wind turbines of $4,000/kW[29]). That 100-year event would rank as one of the ten costliest two-year periods in U.S. history in terms of hurricane damage and the 50-year event would rank as one of the fifteen costliest 2-year periods. For comparison, Hurricane Ike, one of the costliest hurricanes in U.S. history after Katrina, caused approximately $29.5 billion in damages.[6] It is unlikely that the entire Texas coastline will be developed, but the insurance exposure could be in the billions of dollars if there is significant offshore wind power development in the Gulf of Mexico with current wind turbine designs.

To mitigate the risks of hurricanes, offshore wind turbines can be designed for higher maximum wind speeds, designed to track the wind direction (yaw) quickly enough to match wind changes in a hurricane even if grid power is cut off, or placed in areas with lower hurricane risk, as discussed by Rose, *et al.*[17] Efforts are underway to determine design standards for offshore wind turbines in hurricane prone areas[47]. Battery backup is a low-cost way to maintain yawing capability when grid power is interrupted[17]. Nearly all planned offshore wind development in the U.S. in the next 10 – 20 years will occur in low-risk areas such as New England and the Mid-Atlantic states. A U.S Department of Energy report envisions a scenario with 54 GW of offshore wind from North Carolina to Maine by 2030[4] and the U.S. Bureau of Ocean Energy Management (BOEM) is planning to auction offshore wind leases from Massachusetts to Virginia.[48] However, the state of Texas has strongly encouraged onshore wind development and has signed a lease for a wind power development near Galveston[49].

The model developed for this paper uses simulated hurricane tracks and intensities based on climatological conditions from 1979 to 2011; it does not assess the effects of climate change. There has been significant work on evaluating the implications of climate change on hurricane occurrence[21,50-52]. Studies suggest the frequency of hurricanes may not increase in the future and may even decrease, but the intensity of these tropical cyclones is likely to increase as a result of climate change. These conflicting trends will affect the risk hurricanes pose on the large-scale deployment of offshore wind resources in the Gulf Coast, where we find the current risk is the

greatest. While a reduction in hurricane frequency may mean there is a reduction in risk, the increased intensity will result in increased damages by individual storms. It is hard to measure, however, which of these two mechanisms will affect the risk to offshore wind farms the most.

5. ACKNOWLEDGEMENTS

We are very grateful to Kerry Emanuel for providing sets of simulated hurricanes, post-processing routines, and technical support. This work was supported in part by the EPA STAR fellowship program, a grant from the Alfred P. Sloan Foundation and EPRI to the Carnegie Mellon Electricity Industry Center, and by the Doris Duke Charitable Foundation, the R.K. Mellon Foundation and the Heinz Endowments for support of the RenewElec program at Carnegie Mellon University. This research was also supported in part by the Climate and Energy Decision Making (CEDM) center created through a cooperative agreement between the National Science Foundation (SES-0949710) and Carnegie Mellon University

6. REFERENCES

1. Wiser R, Bolinger M. 2011 Wind Technologies Market Report. Oak Ridge, TN: U.S. Department of Energy; 2012 Jul pages 1–93. Report No.: DOE/GO-102012-3472.

2. Schwartz M, Heimiller D, Haymes S, Musial W. Assessment of Offshore Wind Energy Resources for the United States. Golden, CO: National Renewable Energy Laboratory; 2010 Jun pages 1–104. Report No.: NREL/TP-500-45889.

3. OffshoreWind.net [Internet]. offshorewind.net. [cited 2012 Nov 18]. Available from: http://www.offshorewind.net

4. DOE. 20% Wind Energy by 2030. Lindenberg S, Smith B, O'Dell K, DeMeo E, Ram B, editors. U.S. Department of Energy; 2008 Jul pages 1–248. Report No.: DOE/GO-102008-2567.

5. EIA. Electric Power Annual 2010. eia.gov. Washington, DC: U.S. Energy Infomation Administration; 2011 Nov.

6. Blake ES, Landsea CW, Gibney EJ. The Deadliest, Costliest, and Most Intense United States Tropical Cyclones From 1851 to 2010 (and Other Frequently Requested Hurricane Facts). Miami: National Hurricane Center; 2011 Aug pages 1–49. Report No.: NWS NHC-6.

7. Changnon SA. Characteristics of severe Atlantic hurricanes in the United States: 1949–2006. Nat Hazards. Springer; 2009;48(3):329–37.

8. Takahara K, Mekaru T, Shinjo F, Ishihara T, Yamaguchi A, Matsuura S. Damages of wind turbine on Miyakojima Island by Typhoon Maemi in 2003. 2004 European Wind Energy Conference and Exhibition. 2004.

9. Clausen NE, Candelaria A, Gjerding S, Hernando S, Nørgård P, Ott S, et al. Wind farms in regions exposed to tropical cyclones. 2007 European Wind Energy Conference and Exhibition. 2007.

10. Cauffman SA. Performance of Physical Structures in Hurricane Katrina and Hurricane Rita: A Reconnaissance Report. Gaithersburgh, MD: National Institute of Standards and Technology; 2006 Jul pages 1–270. Report No.: NIST Technical Note 1476.

11. Johnson T. New Jersey's Aging Power Plants, Another Casualty of Superstorm Sandy [Internet]. njspotlight.com. 2012 [cited 2012 Nov 18]. Available from: http://www.njspotlight.com/stories/12/11/16/new-jersey-s-aging-power-plants-another-casualty-of-superstorm-sandy/

12. Power Reactor Information System [Internet]. International Atomic Energy Agency; 2012 [cited 2012 Oct 18]. Available from: http://www.iaea.org/pris/CountryStatistics/CountryDetails.aspx?current=JP

13. Sagawa A. Coal for Power Generation: Supply and Demand Following the Great East Japan Earthquake. Institute of Energy Economics, Japan. Tokyo; 2012. pages 1–6.

14. Tsukimori O. Tohoku: Haramachi plant to resume before summer 2013 [Internet]. Reuters. 2012 [cited 2012 Aug 13]. Available from: http://www.reuters.com/article/2012/01/27/japan-power-tohoku-idUST9E7NL01L20120127

15. IEA. IEA Wind 2011 Annual Report. International Energy Agency; 2012 Jul pages 1–5.

16. NERC. 1998 System Disturbances. nerc.com. Princeton, NJ: North American Electric Reliability Council; 2001 May pages 1–44.

17. Rose S, Jaramillo P, Small MJ, Grossmann I, Apt J. Quantifying the hurricane risk to offshore wind turbines. Proceedings of the National Academy of Science. 2012 Feb 28;109(9):3247–52.

18. Powell MD, Cocke S. Hurricane wind fields needed to assess risk to offshore wind farms. Proc Natl Acad Sci U S A. National Acad Sciences; 2012 Aug 14;109(33):E2192–2.

19. Mahdyiar M, Porter B. The Risk Assessment Process: The Role of Catastrophe Modeling in Dealing with Natural Hazards. Grossi P, Kunreuther H, editors. Catastrophe Modeling: A New Approach to Managing Risk. New York: Springer; 2005. pages 45–68.

20. Emanuel KA, Ravela S, Vivant E, Risi C. A statistical deterministic approach to hurricane risk assessment. Bull. Amer. Meteor. Soc. 2006 Mar;87(3):299–314.

21. Emanuel KA, Sundararajan R, WIlliams J. Hurricanes and Global Warming: Results from Downscaling IPCC AR4 Simulations. Bull. Amer. Meteor. Soc. 2008 Mar 1;89(3):347–67.

22. Emanuel KA, Sundararajan R, WIlliams J. Downscaling hurricane climatologies from global models and re-analyses. 28th Conference on Hurricanes and Tropical Meteorology. Orlando;

2008.

23. Holland GJ, Belanger JI, Fritz A. A Revised Model for Radial Profiles of Hurricane Winds. Mon. Wea. Rev. 2010 Dec;138(12):4393–401.

24. Emanuel KA. Personal communication. 2012.

25. Demuth JL, DeMaria M, Knaff JA. Improvement of advanced microwave sounding unit tropical cyclone intensity and size estimation algorithms. Journal of Applied Meteorology and Climatology. 2006;45(11):1573–81.

26. Powell M, Soukup G, Cocke S, Gulati S, Morisseau-Leroy N, Hamid S, et al. State of Florida hurricane loss projection model: Atmospheric science component. Journal of Wind Engineering and Industrial Aerodynamics. 2005 Aug;93(8):651–74.

27. Ho FP, Su JC, Hanevich KL, Smith RJ, Richards FP. NOAA Technical Report NWS 38: Hurricane Climatology for the Atlantic and Gulf Coasts of the United States. Silver Spring, MD: National Weather Service; 1987 Apr pages 1–209. Report No.: NOAA Technical Report NWS 38.

28. Brower M. Development of Eastern Regional Wind Resource and Wind Plant Output Datasets. Golden, CO: National Renewable Energy Laboratory; 2009 Dec. Report No.: NREL/SR-550-46764.

29. Musial W, Ram B. Large-Scale Offshore Wind Power in the United States: Assessment of Opportunities and Barriers, NREL (National Renewable Energy Laboratory). osti.gov. 2010 Sep pages 1–240.

30. Emanuel KA, DesAutels C, Holloway C, Korty R. Environmental control of tropical cyclone intensity. Journal of the Atmospheric Sciences. 2004;61(7):843–58.

31. DeGroot MH, Schervish MJ. Probability and Statistics. 3rd ed. Boston: Addison Wesley; 2002.

32. Willoughby HE, Rahn ME. Parametric Representation of the Primary Hurricane Vortex. Part I: Observations and Evaluation of the Holland (1980) Model. Mon. Wea. Rev. 2004 Dec;132(12):3033–48.

33. Keim BD, Muller RA, Stone GW. Spatiotemporal Patterns and Return Periods of Tropical Storm and Hurricane Strikes from Texas to Maine. J. Climate. 2007 Jul;20(14):3498–509.

34. Emanuel KA, Jagger T. On Estimating Hurricane Return Periods. Journal of Applied Meteorology and Climatology [Internet]. 2010;49(5):837–44. Available from: http://journals.ametsoc.org/doi/abs/10.1175/2009JAMC2236.1

35. Jonkman J, Butterfield S, Musial W, Scott G. Definition of a 5-MW reference wind turbine for offshore system development. Golden, CO: National Renewable Energy Laboratory; 2009 Feb. Report No.: NREL/TP-500-38060.

36. Harper B, Kepert J, Ginger J. Guidelines for converting between various wind averaging periods in tropical cyclone conditions. World Meteorological Organization. Geneva: World Meteorological Organization; 2010 Aug. Report No.: WMO/TD-1555.

37. Sørensen JD, Tarp-Johansen NJ. Reliability-based optimization and optimal reliability level of offshore wind turbines. International Journal of Offshore and Polar Engineering. 2005;15(2):141–6.

38. Gamerman D, Lopes HF. Markov Chain Monte Carlo. 2nd ed. Boca Raton, FL: Chapman & Call/CRC; 2006.

39. Greenwood M. A Report on the Natural Duration of Cancer. Reports on Public Health and Medical Subjects. Ministry of Health. London: UK Ministry of Health; 1926. Report No.: 33.

40. Rose S, Jaramillo P, Small MJ, Grossmann I, Apt J. Reply to Powell and Cocke: On the probability of catastrophic damage to offshore wind farms from hurricanes in the US Gulf Coast. Proc Natl Acad Sci U S A. National Acad Sciences; 2012 Aug 14;109(33):E2193–4.

41. NERC. Standard COM-002-2: Communications and Coordination. nerc.com. Washington, DC; 2007 Jan. Report No.: COM-002-2.

42. ERCOT. ERCOT 10-year outlook indicates need for additional generation. ercot.com. Austin: ERCOT; 2011.

43. Ensslin C, Milligan M, Holttinen H, O'Malley M, Keane A. Current methods to calculate capacity credit of wind power, IEA collaboration. IEEE Power and Energy Society General Meeting. IEEE; 2008. pages 1–3.

44. Hasche B, Keane A, O'Malley M. Capacity Value of Wind Power, Calculation, and Data Requirements: the Irish Power System Case. IEEE Transactions on Power Systems. IEEE; 2011 Feb 1;26(1):420–30.

45. Keane A, Milligan M, Dent CJ, Hasche B, D'Annunzio C, Dragoon K, et al. Capacity Value of Wind Power. IEEE Transactions on Power Systems. 2011;26(2):564–72.

46. Lippert A, Farber-DeAnda M, SeCorla-souza K, Laramey R, Ostrich JTJ, Lewandowski C, et al. Comparing the Impacts of the 2005 and 2008 Hurricanes on U.S. Energy Infrastructure. Washington, DC: US Department of Energy, Office of Electricity Delivery and Energy Reliability; 2009 Feb pages 1–48.

47. Yu Q, Samuelsson L, Tan P-L. Design Considerations for Offshore Wind Turbines in US Waters - The American Way. Houston; 2011. pages 1–13.

48. Brannen P. Offshore wind farms will be encouraged in tracts along the East Coast. Washington Post. Washington, DC; 2012 Jul 23.

49. DOE. Company Plans Large Wind Plant Offshore of Galveston, Texas [Internet]. Energy Efficiency & Renewable Energy Network News. Washington, D.C; [cited 2005 Nov 2]. Available from: http://apps1.eere.energy.gov/news/news_detail.cfm/news_id=9502

50. Knutson TR, McBride JL, Chan J, Emanuel KA, Holland G, Landsea C, et al. Tropical cyclones and climate change. Nat Geosci. 2010 Feb 21;3(3):157–63.

51. Trenberth K. CLIMATE: Uncertainty in Hurricanes and Global Warming. Science. 2005 Jun 17;308(5729):1753–4.

52. Tokdar ST, Grossmann I, Kadane JB, Charest A-S, Small MJ. Impact of Beliefs About Atlantic Tropical Cyclone Detection on Conclusions About Trends in Tropical Cyclone Numbers. Bayesian Analysis. International Society for Bayesian Analysis; 2011;6(4):547–72.

Supporting Information

1. WIND TURBINE PLACEMENT DETAILS

Included Areas:

- Water depth < 30 m
- Mean annual wind speed > 7.4 m/s at 90 m height (http://www.nrel.gov/gis/data_wind.html)
- Distance from shore > 8 km and < 93 km.

Excluded Areas:

Marine Sanctuaries	"Marine Protected Areas" from http://www.cec.org/Page.asp?PageID=924&ContentID=2336
Military Practice Areas	"COASTAL.MIPARE_POLYGON" from http://ocs-spatial.ncd.noaa.gov/SpatialDirect/translationServlet?SSFunction=prepareFetch
Military aviation warning areas	http://www.csc.noaa.gov/ArcGISPUB/rest/services/MultipurposeMarineCadastre/MultipurposeMarineCadastre/MapServer/27/query Filter Geometry: `{xmin: -125, ymin: 29, xmax: -70, ymax: 47}` Geometry Type: `Envelope` Return Fields: `"NAME", "LOWER_ALT"`
Shipping lanes	"COASTAL_FAIRWAY" and "COASTAL_TSEZNE" from http://ocs-spatial.ncd.noaa.gov/SpatialDirect/translationServlet?SSFunction=prepareFetch
Active Oil and Gas Leases	from http://csc.noaa.gov/mmcviewer/
Bays and inland waterways	by hand

2. TOTAL INSTALLED WIND CAPACITY USED IN THIS PAPER

	State	Full Development (MW)
Gulf of Mexico	Texas	86,520
	Louisiana	68,100
Southeast	Georgia	45,740
	South Carolina	21,200
	North Carolina	37,380
Mid-Atlantic	Virginia	15,160
	Maryland	720
	Delaware	6,760
	New Jersey	18,400
	New York	9,940
New England	Rhode Island	3,000
	Massachusetts	29,140
	New Hampshire	40
	Maine	6,840

3. LIFETIME RISK TO A SINGLE WIND FARM

3.1 Additional Results

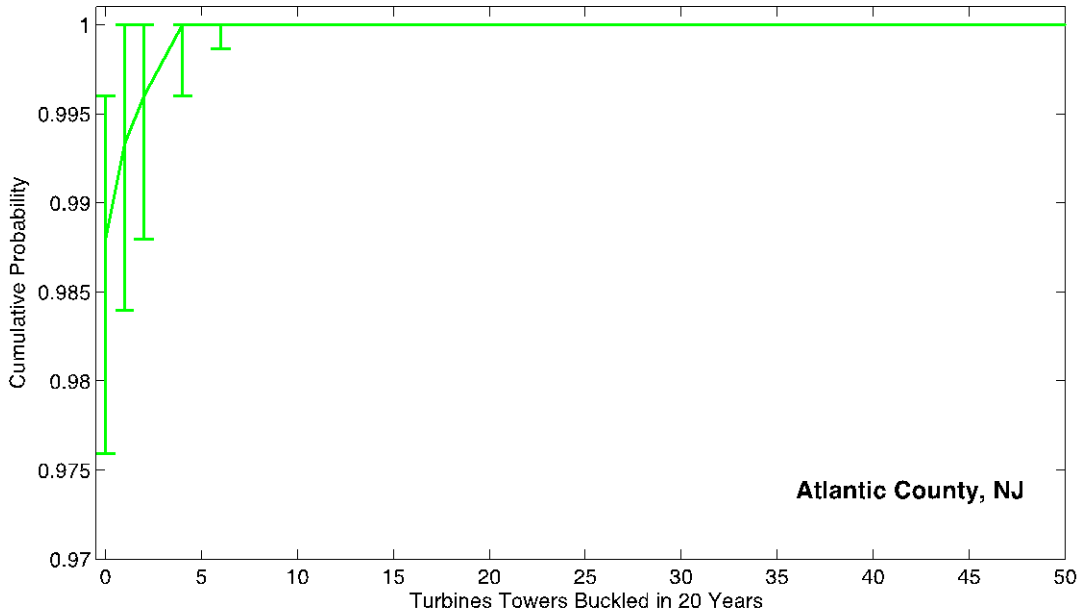

Figure 10: Cumulative distribution of number of turbine towers buckled in Atlantic County, NJ by hurricanes in 20 years if buckled towers are not replaced. Solid lines plot the distribution for the cast that turbines cannot yaw. Results for yawing turbines are not shown because the risks are too small to calculate with the method in this paper.

Table IV: Comparison of results for Atlantic County with no rebuilding of buckled turbines.

Atlantic County, NJ			
		≥ 1 turbine buckled in 20 years	**> 25 turbines buckled in 20 years**
Non-yawing turbine (broadside to wind)	New results (this paper)	0.4 – 2.4%	0%
	Rose, *et al*, corrected(40)	8%	< 0.1%
	Rose, *et al*(17)	15%	1%
Yawing turbine (head-on to wind)	New results (this paper)	0%	0%
	Rose, *et al*, corrected(40)	0.5%	0%
	Rose, *et al*(17)	1%	0%

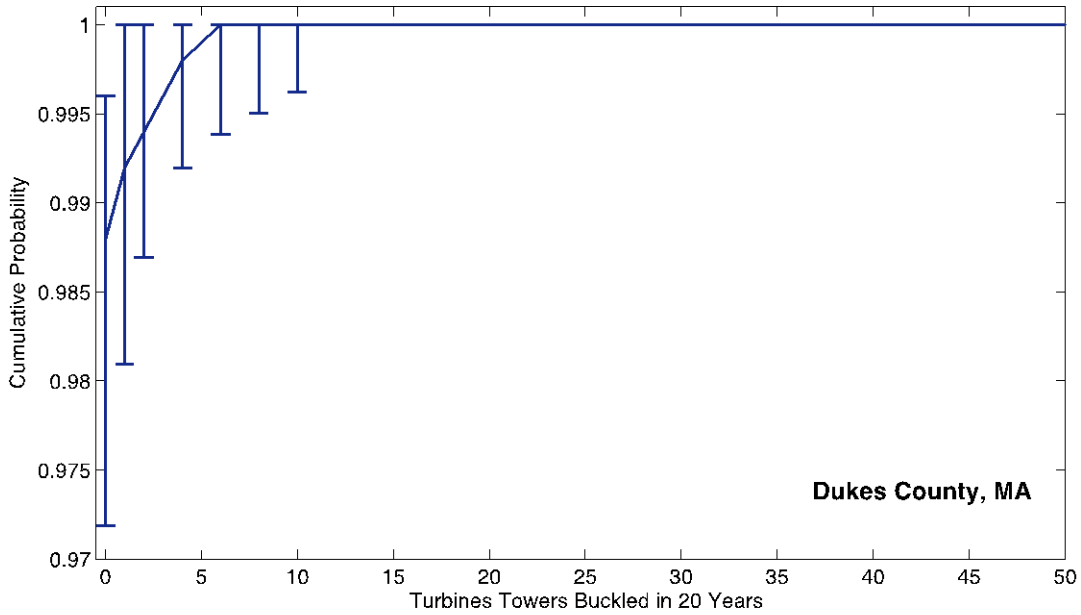

Figure 11: Cumulative distribution of number of turbine towers buckled in Dukes County, MA by hurricanes in 20 years if buckled towers are not replaced. Solid lines plot the distribution for the cast that turbines cannot yaw. Results for yawing turbines are not shown because the risks are too small to calculate with the method in this paper.

Table V: Comparison of results for Dukes County with no rebuilding of buckled turbines.

Dukes County, MA			
		≥ 1 turbine buckled in 20 years	**> 25 turbines buckled in 20 years**
Non-yawing turbine (broadside to wind)	New results (this paper)	0.4 – 2.8%	0%
	Rose, *et al*, corrected(40)	6%	0.1%
	Rose, *et al*(17)	10%	< 1%
Yawing turbine (head-on to wind)	New results (this paper)	0%	0%
	Rose, *et al*, corrected(40)	1%	< 0.1%
	Rose, *et al*(17)	1%	0%

3.2 Wind Farm Locations

	Wind Farm Locations
Galveston County, TX	29.09ºN, 94.90ºW 29.25ºN, 94.71ºW 29.41ºN, 94.41ºW 28.76ºN, 94.63ºW 28.82ºN, 94.32ºW 28.96ºN, 94.18ºW
Dare County, NC	35.09ºN, 75.93ºW 35.21ºN, 75.57ºW 35.50ºN, 75.34ºW 35.73ºN, 75.41ºW 36.17ºN, 75.61ºW
Atlantic County, NJ	39.24ºN, 74.34ºW 39.31ºN, 74.26ºW 39.40ºN, 74.24ºW
Dukes County, MA	41.45ºN, 70.96ºW 41.23ºN, 70.73ºW 41.27ºN, 70.42ºW 41.48ºN, 70.37ºW

4. DAMAGE FUNCTION

4.1 Metropolis-Hastings Algorithm

We use a Metropolis-Hastings algorithm (a special case of Markov Chain Monte Carlo methods) to estimate the three parameters $\theta_1 = \alpha$, $\theta_2 = \beta$, $\theta_3 = \sigma$ for the turbine damage function. Specifically, we use the Metropolis-Hastings algorithm with component wise updating of the parameters(38), according to the following steps:

1. Initialize an iteration counter $j = 1$ and set initial values of the parameters $\boldsymbol{\theta}^{(0)}$. It helps to choose initial parameter values relatively close to the expected final values because the NH algorithm will converge faster that way.
2. For each parameter θ_i:
    a. Propose a new parameter value θ_i^* as a function of the previous parameter value $\theta_i^{(j-1)}$ according to the proposal distribution q:

$$\theta_i^* \sim q\left(\theta_i^{(j)} | \theta_i^{(j-1)}\right) = \text{Gamma}\left(\tau_i \theta_i^{(j-1)},\ 1/\tau_i\right)$$

b. Calculate the proposal ratio:

$$\text{prop. ratio} = \frac{q\left(\theta_i^{(j-1)} | \theta_i^*\right)}{q\left(\theta_i^* | \theta_i^{(j-1)}\right)}$$

c. Calculate the likelihood ratio, which is the ratio of the likelihood function with 3 parameters: the proposed value for the i^{th} parameter θ_i^* and the values for the two other parameters from the previous step $\theta_{\neg i}^{(j-1)}$:

$$\text{like. ratio} = \frac{p\left(\theta_i^*,\ \theta_{\neg i}^{(j-1)}\right)}{p\left(\theta_i^{(j-1)},\ \theta_{\neg i}^{(j-1)}\right)}$$

where the likelihood function based on equation (4) in the body of the paper is the product of the probability density value of the residuals (difference between measured turbine buckling probability and loglogistic model) for the K measured turbine buckling probabilities $y(u_k)$ that are a function of wind speed u_k: For example:

$$p(\theta_2^*, \theta_{-2}^{(j-1)}) = p(\theta_1^{(j-1)}, \theta_2^*, \theta_3^{(j-1)})$$

$$= \prod_{k-1}^{K} f\left(\left(y(u_k) - \text{loglogistic}(u_k; \alpha^{(j-1)}, \beta^*)\right);\ 0, \sigma_D^{(j-1)}\right)$$

where f(x; μ, σ) is the PDF of the Normal distribution:

$$f(x;\ \mu, \sigma) = \frac{1}{\sqrt{2\pi\sigma^2}} \exp\left(\frac{-(x-\mu)^2}{2\sigma^2}\right)$$

d. Calculate the acceptance probability α as the minimum of the proposal ration and the likelihood ratio:

$$\alpha = \min\{1, \text{prop. ratio}, \text{like. ratio}\}$$

e. If the proposal is accepted (α > uniform random number), $\theta_i^{(j)} = \theta_i^*$, otherwise $\theta_i^{(j)} = \theta_i^{(j-1)}$ and go to the next parameter θ_{i+1}

3. Increment the iteration counter $j = j+1$

In the Gamma distribution in step 2a, τ is a parameter that must be tuned to improve the convergence speed of the algorithm; we set $\tau_\alpha = 100$, $\tau_\beta = 5$, and $\tau_{\sigma D} = 1000$. In the likelihood function in step 2c, y_k is the simulated probability of tower buckling at wind speed u_k. Each pair (u_k, y_k) corresponds to a point in Figure 7. We simulated turbine buckling at $K = 36$ different 10-min average wind speeds from 77.6 – 213.8 knots (40 – 110 m/s, in 2 m/s steps). The details of the turbine buckling simulation are given in the Supporting Information of work by Rose, *et al.* (17)

We assume informationless priors, i.e. uniform distributions.

5. MODEL VALIDATION

Emanuel, *et al,* have shown that the simulated hurricanes we use as the basis for our analysis have statistical properties similar to historical hurricanes.(20) However, we transform those simulated hurricanes by modeling uncertainty in their return rate and size. We validate the

transformed hurricanes by calculating the return periods of three different storm intensities at 45 locations along the U.S. coast (Section 4.1 below) and return periods of a range of wind speeds in New Orleans and Miami (Section 4.2 below).

5.1 Return Period of Storms Along the U.S. Coast

We estimate return periods of intense hurricanes, all hurricanes, and all tropical storms for 45 points along the Gulf and Atlantic coasts using the simulated hurricanes described in the body of the paper. For each point, the return periods are calculated within 20 km of the point for storms that pass within 240 km of the point, using the simulated hurricanes described in the body of the paper. We present these results for comparison with results based on historical hurricane data in a paper by Keim, *et al.*(33)

In Figure 10 we plot our estimates of the return periods of winds greater than intense-hurricane (> 96 knots), which are comparable to the historically-based return periods given by Keim, *et al* for most locations. This is important because offshore wind turbine designed to existing standards are most vulnerable to intense hurricanes. Our simulations predict shorter return periods for intense-hurricane-force winds along the coasts of Georgia, northeastern Florida, and northwestern Florida, but the historical record is not long enough to accurately estimate return periods for those regions.

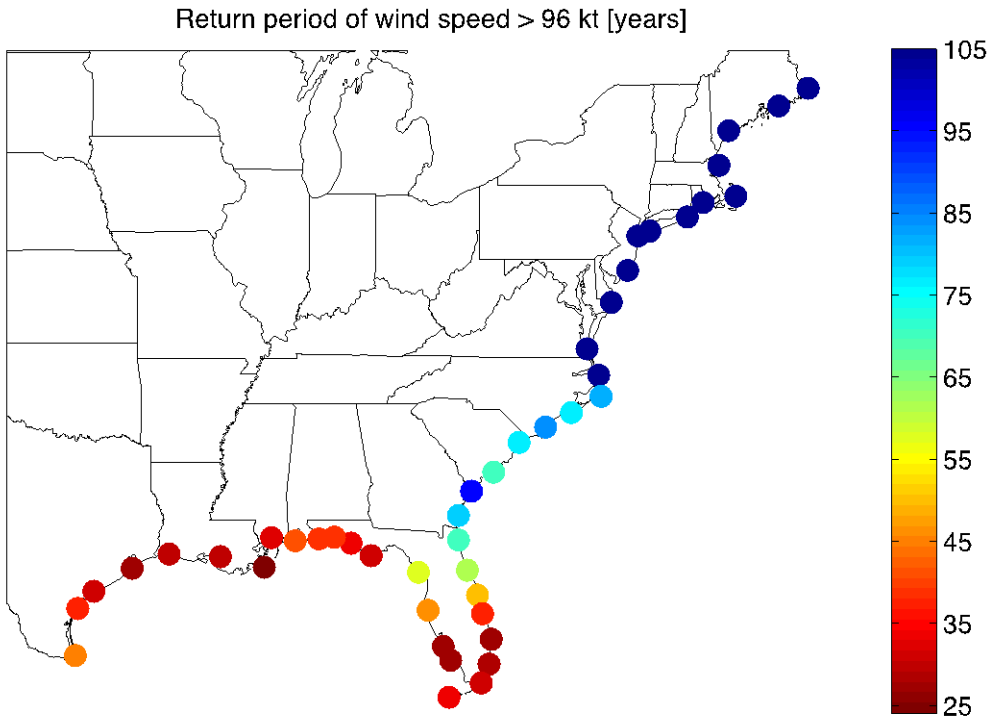

Figure 12: Return periods of wind speeds greater than 96 knots (intense hurricanes) within 20 km of each point, calculated with the simulation method described in the body of the paper.

In Figure 11 we plot our estimates of return periods for winds greater than hurricanes strength (> 64 knots), which predict shorter return periods than the historical record. Although our results over-predict the frequency of all hurricanes relative to historical data, we expect this has little effect on our turbine risk results because most of risk comes from intense hurricanes and we show in Figure 10 that we model the return period of those well.

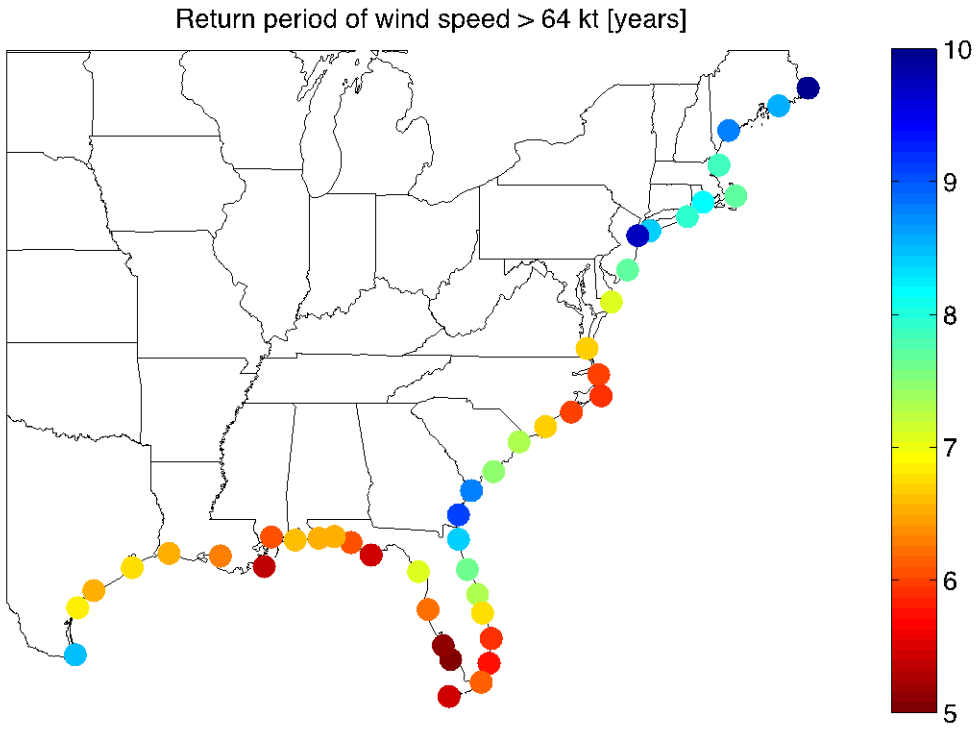

Figure 13: Return period of wind speeds greater than 64 knots (hurricanes) within 20 km of each point, calculated with the simulation method described in the body of the paper.

In Figure 12 we plot our estimates of return periods for tropical-storm-force winds, which predict shorter return periods than the historical record. As with the return periods of all hurricanes in Figure 11, we expect this has little effect on our turbine risk results because most of risk comes from intense hurricanes and we show in Figure 10 that we model the return period of those well.

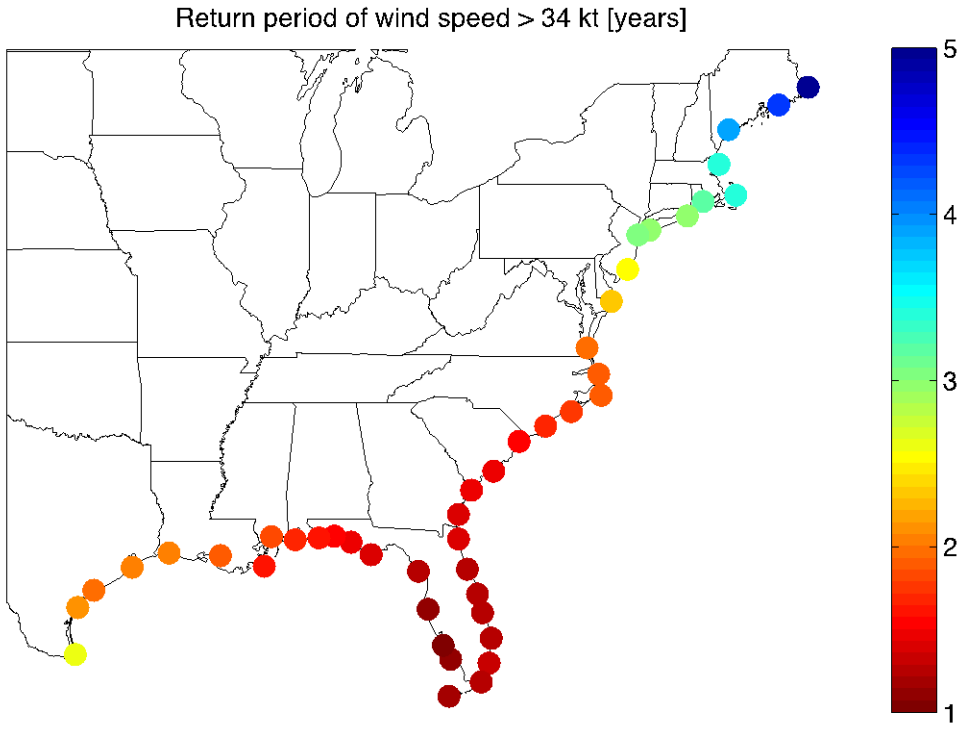

Figure 14: Return period of wind speeds greater than 34 knots (tropical storms) within 20 km of each point, calculated with the simulation method described in the body of the paper.

5.2 Return Periods of Maximum Total Wind Speed for Select Locations

We estimate the distribution of return periods for a range of maximum total wind speeds for New Orleans and Miami, shown in Figure 13 and Figure 14. For each point of interest, the return periods are calculated within 100 km of the point for storms that pass within 100 km of the point, using the simulated hurricanes described in the body of the paper. We present these results for comparison with results based on historical hurricane data in a paper by Emanuel and Jagger.(33)

We find the return periods we estimate for total maximum wind speed in New Orleans (Figure 13) are somewhat shorter than the return periods Emanuel and Jagger estimate. For example we estimate 100-knot winds have approximately a 25-year return period but Emanuel and Jagger estimate approximately 30 years. We estimate 120-knot winds have a return period of approximately 45 years but Emanuel and Jagger estimate approximately 65 years. Both our estimates and Emanuel and Jagger's both fall within the confidence interval for return periods estimated from historical hurricane records. We believe our estimates differ from Emanuel and Jagger's even though we use the same model to simulate hurricanes because our hurricanes are have larger radii of maximum winds that better match the distribution of sizes of historical hurricanes.

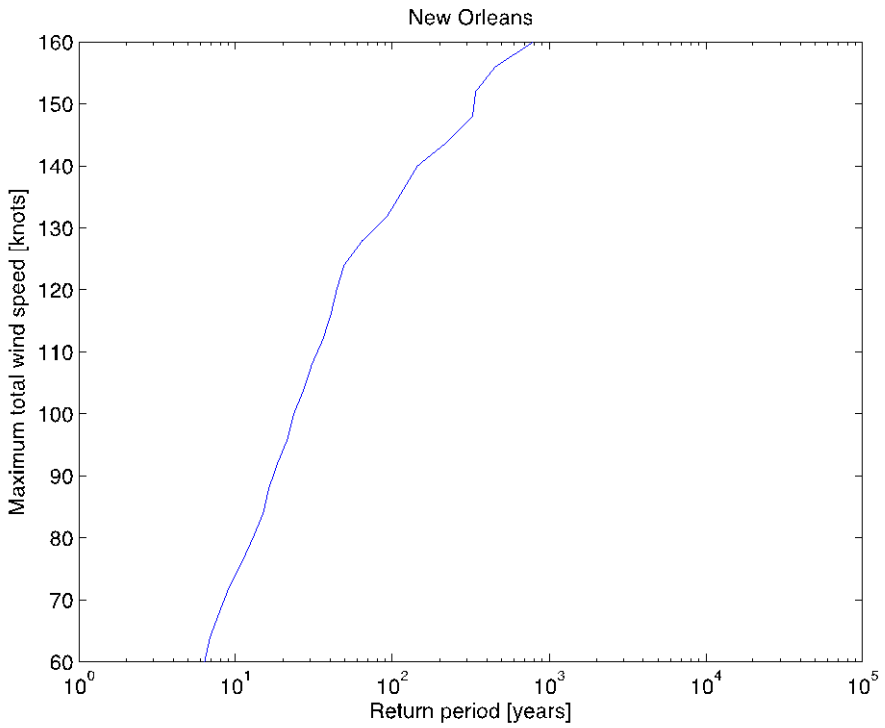

Figure 15: Return periods for maximum total wind speeds within 100 km of New Orleans, calculated from the simulated hurricanes described in the body of the paper.

We find the return periods we estimate for total maximum wind speed in Miami (Figure 14) are somewhat different from the return periods Emanuel and Jagger estimate. For example we estimate 100-knot winds have approximately a 24-year return period but Emanuel and Jagger estimate approximately 17 years. We estimate 120-knot winds have a return period of approximately 55 years but Emanuel and Jagger estimate approximately 38 years. Both our estimates and Emanuel and Jagger's both fall within the confidence interval for return periods estimated from historical hurricane records.

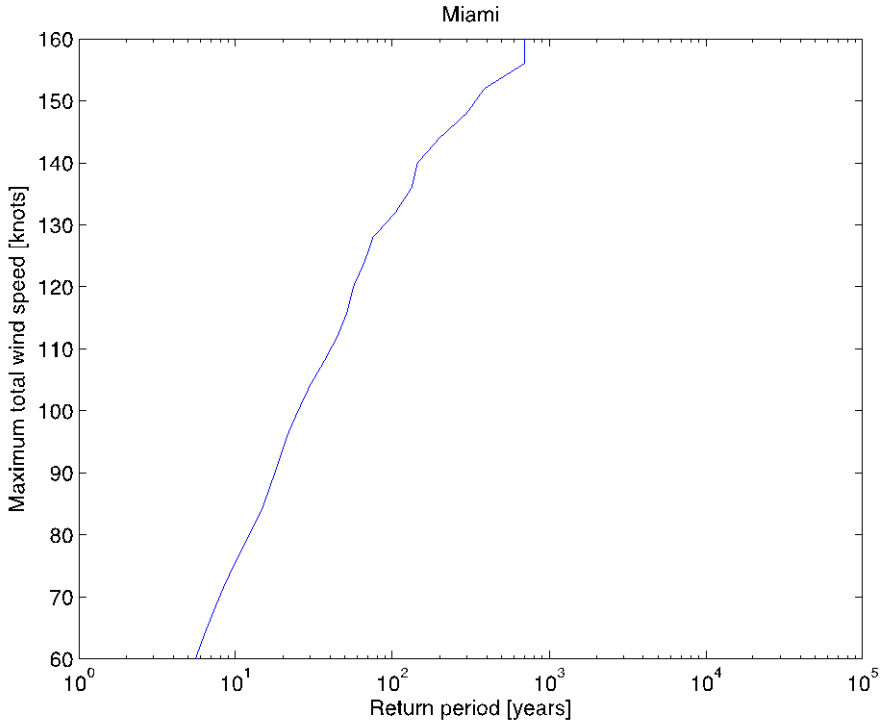

Figure 16: Return periods for maximum total wind speeds within 100 km of Miami, calculated from the simulated hurricanes described in the body of the paper.